- Technical Paper -

FEM Analysis of the Shear Behavior of Short RC Columns Subjected to Lateral Cyclic Loading

Ionut Ovidiu TOMA[*1], Toshihide KIMURA[*2], Ken WATANABE[*3] and Junichiro NIWA[*4]

ABSTRACT

A series of three short RC columns containing conventional reinforcement and 1% steel fibers were subjected to cyclic loading until shear failure. The columns had different shear reinforcement ratios in order to account for its effect on the behavior of RC columns subjected to cyclic loading. A 2D nonlinear FEM analysis was also performed to model the behavior of the tested specimens. The increase in the shear reinforcement ratio results in a slight increase in the resisted peak load and in a larger energy dissipation. The FEM analysis can predict the resisting peak load with good accuracy.

Keywords: short columns, steel fibers, shear failure, FEM analysis

1. INTRODUCTION

During recent seismic events, it was observed that the failure of reinforced concrete structures was closely related to the occurrence of the shear failure of columns. The types of columns that are more susceptible to the shear failure are short columns. Even though, recently, the construction of such columns in seismically active areas has been avoided, there are still a large number of buildings that have short columns as a part of their structure.

Columns built following the old codes have been designed to resist mainly flexure. However, there were cases when an abrupt non-ductile failure of short columns occurred before their flexural strength was reached. Brittle shear failure reduces the energy dissipating capacity of the columns compared to a more ductile flexural failure. Because of that design codes specify shear reinforcement placing methods in order to prevent such brittle failure. However, densely placed reinforcement might make the casting of concrete very difficult and possibly result in large gaps inside the concrete members.

The addition of steel fibers can significantly improve the engineering properties of concrete, notably the shear strength [1]. It also increases the fatigue strength and the resistance to cracking. Even in already damaged concrete members, the presence of steel fibers can improve the structural behavior of such members compared to conventionally reinforced concrete structural members [2].

Recently, the numerical simulations of the experimental procedures have shown an increasing trend. The necessity of having good FEM models that can match the experimental results is of paramount importance. The benefits of using FEM analysis are manifold: shorter time until the results are obtained, the parameters can be easily changed in order to assess their influence on the behavior of analyzed structural members, etc.

The present study focuses on the shear carrying capacity and shear behavior of short reinforced concrete columns containing both conventional reinforcement and steel fibers, subjected to lateral cyclic loading. The increase of the shear reinforcement ratio r_w, results in an increase in the peak resisting load and in the energy dissipation capacity of the columns. The numerical simulations give reasonable agreement with the experimental results in terms of the peak resisting load. However, the ductile post peak behavior of the columns could not be captured by the nonlinear FEM analysis with sufficient accuracy.

2. MATERIALS

2.1 Concrete

For this study, a concrete with a design compressive strength of 30 N/mm^2, obtained from uniaxial compression tests at 7 days according to JIS A 1108, was considered. The compressive strength of each batch cast using the concrete mix proportion shown in Table 1 was measured at the day of testing.

2.2 Reinforcement

The longitudinal reinforcement used in this study was of deformed type, D22 SPBD1170, with the area of the bar equal to A_s = 387.1 mm^2. The yield strength of the longitudinal reinforcement was measured and the value was f_y = 1198 N/mm^2.

The shear reinforcement was also of deformed type, D6 SD295, with the area of the bar equal to A_s = 31.67 mm^2. The yield strength of the shear

*1 Dr. Eng., Dept. of Civil Engineering, Tokyo Institute of Technology, JCI Member.
*2 Graduate Student, Dept. of Civil Engineering, Tokyo Institute of Technology, JCI Member.
*3 Assistant Professor, Ph.D., Dept. of Civil Engineering, Tokyo Institute of Technology, JCI Member.
*4 Professor, Dr. Eng., Dept. of Civil Engineering, Tokyo Institute of Technology, JCI Member.

Table 1 Concrete mix proportion

Concrete Mix	W/C (%)	s/a (%)	W*1 (kg/m^3)	C*2 (kg/m^3)	S*3 (kg/m^3)	G*4 (kg/m^3)	Admixture*5 (%)
F10R00 F10R21 F10R42	55	47	172	314	838	950	0.3

*1 Water; *2 High early strength Portland Cement, specific gravity = 3.14; *3 Sand; *4 Coarse aggregate, G_{max} = 20 mm; *4 Air entraining and water reducing admixture, percentage of the cement mass.

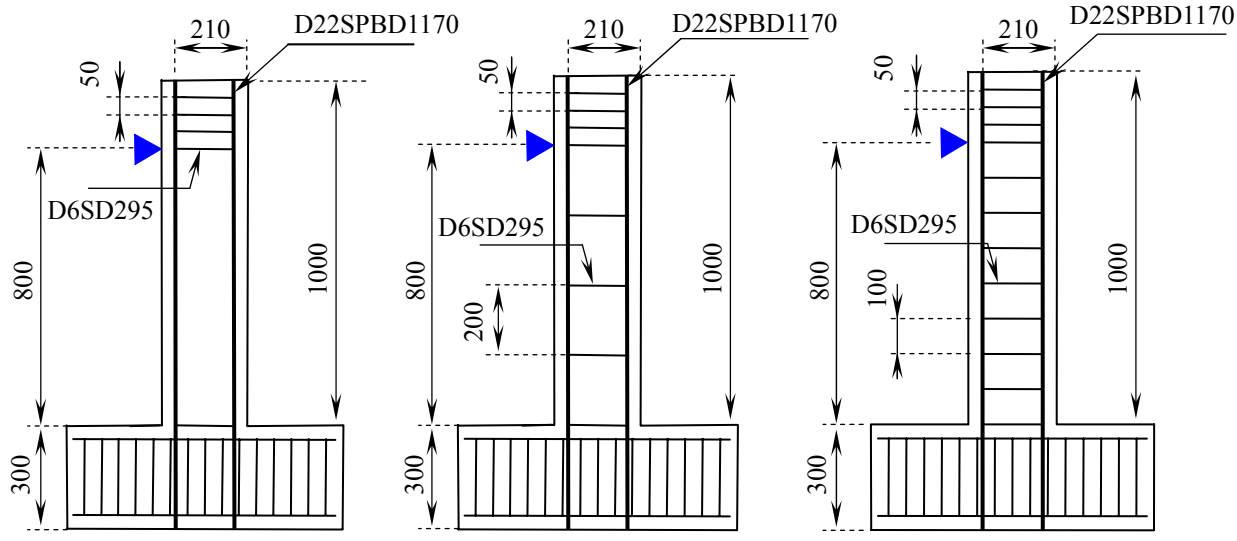

(a) F10R00 (b) F10R21 (c) F10R42

Fig.1 Specimen geometry and reinforcement layout (unit: mm)

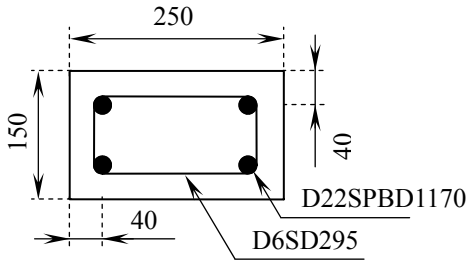

Fig.2 Cross sectional dimensions (unit: mm)

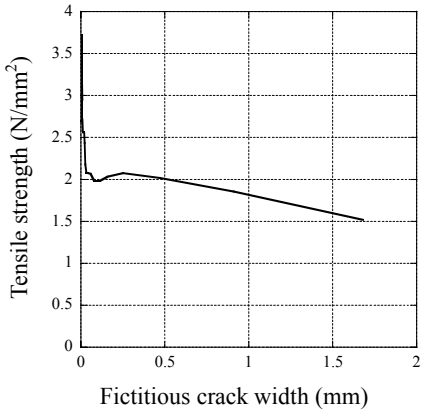

Fig.3 Tension softening curve

reinforcement was also measured and the value was f_y = 350 N/mm^2.

2.3 Steel fibers

The steel fibers used in this study were with crimped ends. The length is L_f = 30 mm and the diameter is d_f = 0.6 mm, giving an aspect ratio of L_f/d_f = 50. The ultimate tensile strength f_u is 1000 N/mm^2 and the elastic modulus E is 2.1×10^5 N/mm^2.

Table 2 Material properties of concrete

Concrete Mix	Compressive Strength*1 N/mm^2	Tensile Strength*2 N/mm^2	Elastic Modulus N/mm^2
F10R00	36.1	3.5	28600
F10R21	36.6	3.2	28100
F10R42	38.7	3.2	28100

*1 Measured according to JIS A 1108
*2 Measured according to JIS A 1113

Table 3 Material properties of conventional reinforcement

Reinforcement name	Type	Yield Strength N/mm^2
Transverse	D6 SD295	350
Longitudinal	D22 SPBD1170	1198

3. TEST PROGRAM

3.1 Experimental procedure

The specimens presented in this paper are a part of a larger experimental program on short RC columns with various percentages of steel fibers, subjected to lateral cyclic loading. They were selected in order to assess the influence of the shear reinforcement ratio, r_w, on the behavior of the columns.

The reinforcement layouts of the test specimens are presented in Figs. 1(a), 1(b) and 1(c). Figure 2 shows the cross section of the columns. For all the specimens, the shear span by the effective depth ratio,

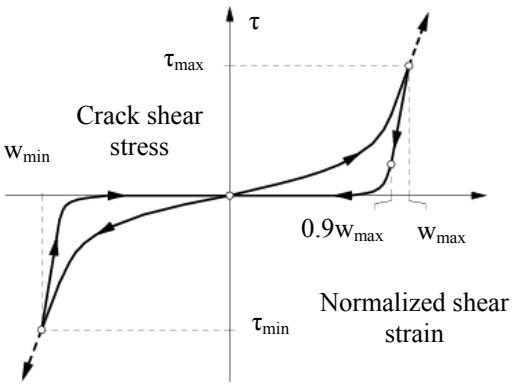

Fig.4 Hysteretic model of stress-strain relationship

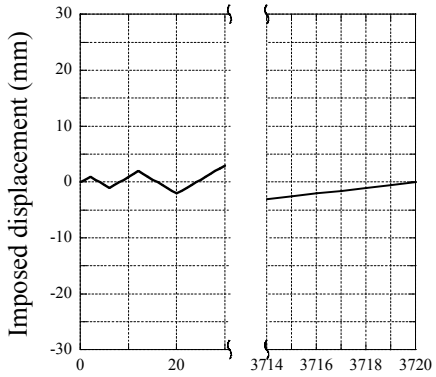

Fig.5 Loading diagram for the FEM analysis

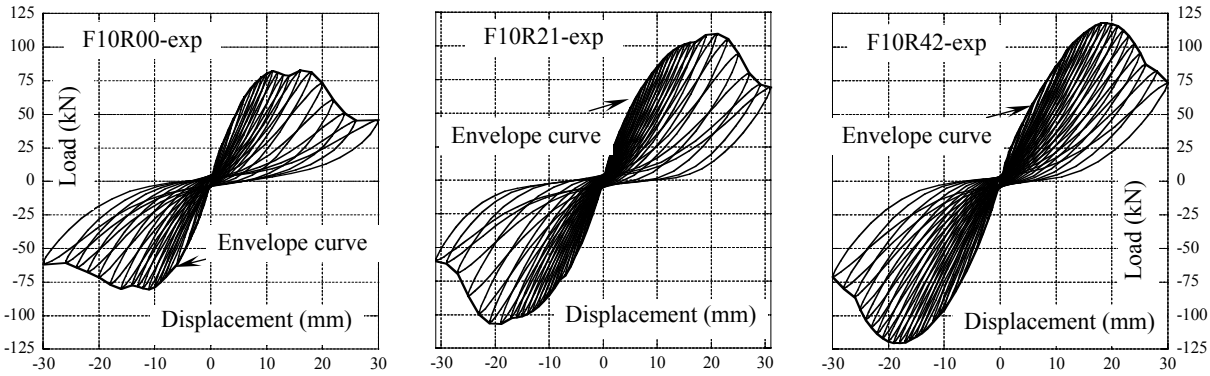

Fig.6 Load-displacement diagrams for the tested specimens (experimental results)

a/d, was 3.81. The longitudinal reinforcement ratio, p_w, was also kept constant for all the columns and the value was set to 2.49%. The high value for p_w was chosen to ensure the occurrence of shear failure. The specimens were denoted according to the contained percentage of steel fiber and their shear reinforcement ratio. Hence, F10R21 means that the column has 1.0% steel fibers and the shear reinforcement ratio is 0.21%.

3.2 FEM analysis

A two dimensional non-linear FEM analysis was conducted by means of DIANA program. The columns and the footings were modeled using 4-node plane stress elements. The reinforcement was modeled by means of embedded reinforcement elements. Because of this, the slip between the longitudinal reinforcement and the concrete is neglected at this stage. The values of the material properties for the concrete and the conventional reinforcement were obtained experimentally and are summarized in Tables 2 and 3, respectively.

The concrete was modeled using Thorenfeldt [3] model for the compression region. For the tensile regime, the tension-softening curve showed in Fig. 3 was used [4]. It was used via the MULTLN function in DIANA software that allows the user to define up to 30 points in terms of tensile stress and strain. The shear retention function was adopted according to Maekawa et al. [5]. The function is based on the contact density model that defines a nonlinear relationship between the normalized shear strain (w) and the crack shear stress (τ). The governing equation has various parameters and is different for loading and unloading/reloading, depending on the value of the normalized shear strain. The latter depends on the crack shear strain and the crack opening. The hysteretic model of the stress-strain relationship is presented in Fig. 4, according to DIANA user manual. The closing of the formed cracks on the unloading stages was also considered. This means that the gradual increases in stresses at the faces of the cracks are taken into account in the finite element analysis.

The models were loaded by using imposed displacements according to the diagram shown in Fig. 5. The displacement increment was 0.5 mm. The specimens were loaded until the maximum displacement of 30 mm obtained in the experiment was reached. The iteration procedure was controlled in terms of relative energy variation with a tolerance of 10^{-5}. The loading diagram presented in Fig. 4 was similar to the actual loading steps used in the experimental procedure.

4. RESULTS AND DISCUSSIONS

4.1 Load-displacement curves

Figure 6 presents the load-displacement diagrams for the tested columns with the data obtained from the loading tests. From the envelope curves (the bold lines joining the values of the load corresponding to the maximum displacement according to each loading step) it can be observed that there are no sudden drops in the load even in the post peak region. This is due to the fact that steel fibers were used in the

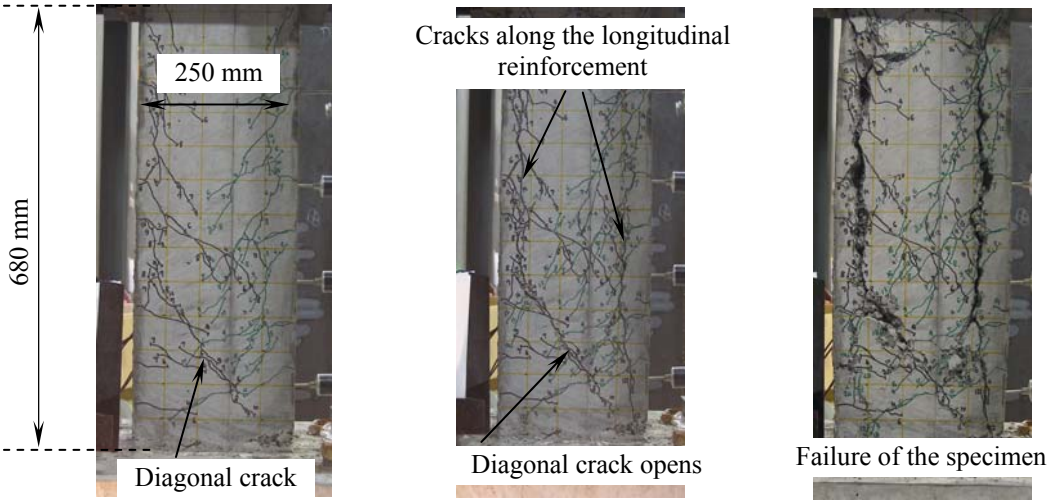

(a) Formation of the diagonal crack (b) Diagonal crack opening (c) Failure of the specimen

Fig.7 Failure stages of F10R00

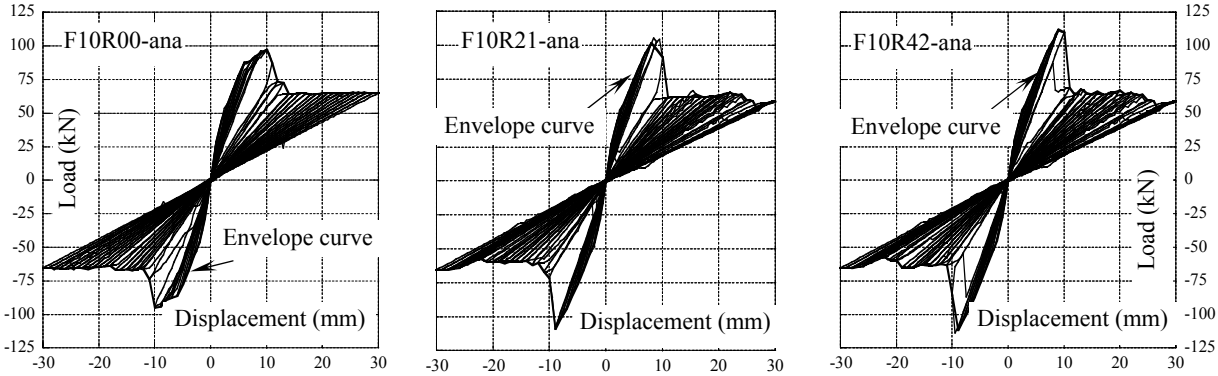

Fig 8 Load displacement curves for the tested specimens (analytical results)

mix proportion.

Specimen F10R00 exhibited a first peak at a displacement of ±10 mm that was consistent with the complete formation of the first diagonal crack, Fig. 7(a). By the time the displacement reached ±16 mm a second peak was recorded, corresponding to the opening of the existing diagonal crack and to the full propagation of the cracks along the longitudinal reinforcement, Fig. 7(b). From this point on, the load decreased continuously until the complete failure is reached at a displacement of ±30 mm, Fig. 7(c). In this study, the load corresponding to the failure of the columns was considered to be 0.6 $\times P_{max}$. It should be noted that even though the specimen was heavily damaged with large crack openings and debonding of the longitudinal reinforcement, the cover concrete did not spall. The benefit from adding steel fibers can be easily observed. This would be of great importance for structures located in areas where severe earthquakes could occur.

Fig 8 shows the load-displacement curves obtained from the FEM analysis. All analyzed cases exhibit slightly increased initial stiffness compared to the tested specimens. The post-peak behavior however shows a sudden drop in the load followed by an almost horizontal region.

Such a different behavior could be explained by the material models that were used in this study. Because steel fiber reinforced concrete is a rather new material and has been in use only in a rather small number of cases for the past decade, there is only a limited number of data available. The tension-softening behavior shown in Fig. 3 even though it was obtained from a limited number of experimental results showed good agreement with the results obtained from subsequent tests. However, the compressive behavior of the steel fiber reinforced concrete (SFRC) has not been studied so extensively. A further difference may come from the lack of considering the effect of steel fibers in the shear retention model [5]. Further study in these particular fields should be conducted in order to improve the FEM analysis results when it comes to SFRC.

Even though the post peak behavior could not be captured using the FEM analysis, the cracking condition can be simulated. Fig. 9 shows a comparison between the cracking condition obtained from the experiment and the analysis for the case of F10R00 at a displacement of ±10 mm, corresponding to the formation of the first diagonal crack.

4.2 Influence of shear reinforcement

Looking at Fig. 6 it can be noticed that F10R21 and F10R42 did show a slightly different behavior.

They both reached their peak loads at a displacement of around ±20 mm. At the same, the peak load increased from 82.97 kN for F10R00 to 109.15 kN and 118 kN for F10R21 and F10R42, respectively.

This can be explained by the confining effect of the shear reinforcement on the core concrete of the column by preventing the excessive deformation of the longitudinal reinforcement at large lateral displacements [6]. Even though the web reinforcement ratio is rather small for the specimen F10R21, its effect is increased by the presence of steel fibers. A further increase in the shear reinforcement ratio from 0.21% to 0.42% has little effect on the peak resisting load or on the maximum displacement for which $0.6 \times P_{max}$ is reached.

On the other hand, the presence of the shear reinforcement has a more significant effect on the dissipated hysteretic energy, as it will be shown in the subsequent section.

4.3 Peak load and dissipated hysteretic energy

Table 4 summarizes the peak resisting loads of the specimens tested in this study. It can be seen that the FEM analysis provides good agreement with the experimental results. Similar to the experiment, the analytical results show a significant improvement in the peak load when web reinforcement is used. However, increasing the shear reinforcement ratio has little influence on the peak load: doubling the value of r_w from 0.21% to 0.42% results only in a 1.1% increase in the peak load for the experimental results and in a 1.07% increase for the results obtained using FEM analysis.

The improvement becomes clearer if the dissipated hysteretic energy is taken into account. The higher the dissipated energy for a structural member is, the better it behaves during a seismic excitation. The energy dissipation capacity is an important parameter in the design of short-period structures and structures subjected to long-duration earthquakes.

The dissipated energy was calculated according to the following equation:

$$E_{hyst} = \sum_{i=1}^{n} E_i \tag{1}$$

where n is the number of cycles (in this case 30) and E_i is the energy (kN×mm) dissipated in each cycle i. E_i can be computed as the area between the loading and the unloading curve for both positive and negative ranges [7].

The calculated results are summarized in Table 5. A closer look at the values of E_{hyst} obtained from the experiment confirms the influence of the web reinforcement on the dissipated hysteretic energy. The results are in agreement with the load-displacement diagrams shown in Fig. 6. Specimens F10R21 and F10R42 exhibit higher peak loads than F10R00. On the other hand, the post peak behavior of F10R42 shows a slower decrease in the load compared to F10R21. Since all specimens contain steel fibers, the benefit comes from the use of shear reinforcement.

On the other hand the results obtained from FEM analysis show only slight differences between the specimens with or without shear reinforcement. Looking at Fig. 8 it can be observed that the unloading path is almost similar to the loading curve. Consequently, the area between these curves is very small and so is the energy dissipated during a single

Table 4 Experimental results vs. analytical results

Specimen	$P_{\max}^{\exp}$ (kN)	$P_{\max}^{ana}$ (kN)	$P_{\min}^{\exp}$ (kN)	$P_{\min}^{ana}$ (kN)	$P_{\max}^{\exp} / P_{\max}^{ana}$	$P_{\min}^{\exp} / P_{\min}^{ana}$
F10R00	82.97	97.4	-80.3	-95.06	0.85	0.84
F10R21	109.15	105.2	-106.8	-108.8	1.04	0.98
F10R42	118	112.5	-120.2	-113.6	1.05	1.06

Table 5 Dissipated hysteretic energy

Specimen	$E_{hyst}^{\exp}$ (kN×mm)	E_{hyst}^{ana} (kN×mm)
F10R00	4.45×10^3	2.21×10^3
F10R21	6.75×10^3	2.54×10^3
F10R42	7.75×10^3	2.63×10^3

Table 6 Ductility factor

Specimen	Ductility factor μ	
	Experiment	Analysis
F10R00	1.63	1.9
F10R21	1.55	2.0
F10R42	1.58	1.2

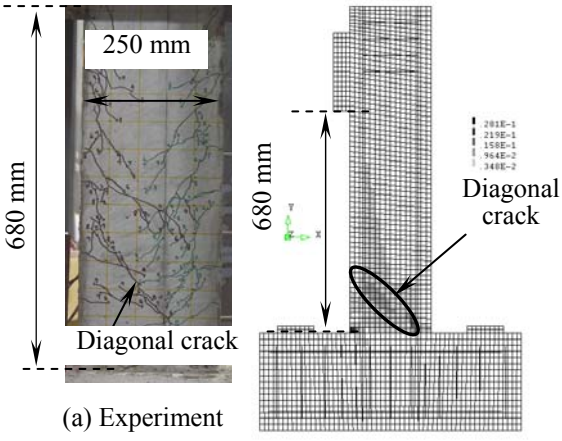

(a) Experiment

(b) Principal tensile strains (FEM analysis)

Fig. 9 First diagonal crack for F10R00 (experiment and analysis)

cycle.

4.4 Ductility factor

The response of columns to seismic excitations can be also quantified in terms of the ductility factor. In the seismic design the elastic deformations are generally quantified by ductility parameters and by energy dissipation capacity.

In this paper, the ductility factor is defined as:

$$\mu = \frac{\Delta_u}{\Delta_p} \tag{2}$$

in which Δ_p is the displacement corresponding to the peak load (mm) and Δ_u is the displacement (mm) corresponding to the ultimate resisting load. The column is considered to have failed when the lateral load reaches a value equal to $0.6 \times P_{max}$.

An alternate definition of the ductility factor is in terms of the displacement corresponding to the yielding of the longitudinal reinforcement, Δ_{yl}, and Δ_u [7]. Since one of the objectives of this research was to study the shear behavior of RC columns, a large value of the longitudinal reinforcement ratio p_w was set.

The calculated values of the ductility factor, according to Eq. 2, are summarized in Table 6 both for the experiment and the analysis. According to Eq. 2, a very ductile structural member would reach the peak load at a very small displacement. The curve in the post peak region would have to have a very lean slope to allow for a very large value of Δ_u.

Looking at the values presented in Table 6 for the experiment, it can be seen that F10R00 has the highest ductility factor, reaching the peak load at a displacement of ± 16 mm and $0.6 \times P_{max}$ at a displacement of ± 26 mm. The other two specimens, F10R21 and F10R42 have comparable values of the ductility factor. They both reached the peak load at a displacement $\Delta_p \simeq \pm 20$ mm. This was mainly due to the increased stiffness of the columns caused by the presence of shear reinforcement. It can also be observed that increasing the value of r_w has only a slight effect on the ductility factor as compared to its effect on the dissipated hysteretic energy.

A similar tendency could be observed for the analytical results. According to the calculated values of μ, the specimen F10R00 is more ductile than F10R42. When it comes to F10R21, the value of the ductility factor is on a par with the value obtained for F10R00 and largely overestimating the experimental result. The cause of this spurious result is believed to be the lack of accurate material models for simulating the behavior of fiber reinforced concrete.

5. CONCLUSIONS

(1) Using steel fibers led to an improved performance of short reinforced concrete columns under lateral cyclic loading. Even the specimen without web reinforcement showed a large value of the dissipated energy. On the other hand, the specimen exhibits a ductile post peak behavior. Short steel fiber can be a good counter-measure against brittle failure of short columns located in seismically active areas.

(2) In addition to fibers, shear reinforcement ratio plays also an important role on the overall behavior of concrete columns. Due to the confining effect on the core concrete, columns with a higher shear reinforcement ratio can withstand larger lateral displacements. However, increasing the amount of shear reinforcement ratio has little influence on the peak resisting loads of the specimens tested in this study.

(3) FEM analysis is also employed in the present research work. The analytical results show good agreement with the experimental values in terms of peak resisting loads. On the other hand, the post peak behavior of the columns observed during the experiments could not be captured by means of FEM analysis. Further studies should be conducted in order to obtain more accurate models for the steel fiber reinforced concrete that can be used in conjunction with FEM programs.

REFERENCES

[1] R.N. Swamy, R. Jones and A.T.P. Chiam: Influence of steel fibers on the shear resistance of lightweight concrete T-Beams, ACI Structural Journal, Vol. 90, No. 1, pp. 103-114, 1993

[2] I.O. Toma, T. Miki and J. Niwa: Influence of random cracks on the behavior of reinforced concrete beams containing steel fibers, Journal of Materials, Concrete Structures and Pavements, JSCE, Vol. 63, No. 1, pp. 66-78, 2007

[3] E. Thorenfeldt, A. Tomaszewicz and J.J. Jensen: Mechanical properties of high-strength concrete and applications in design, Proceedings of the Symposium on the Utilization of High-Strength Concrete, Stavanger, Norway, 1987

[4] I. Odera: Mechanical properties of hybrid short fiber reinforcedc concrete using steel and synthetic fibers, Master thesis, Department of Civil Engineering, Tokyo Institute of Technology, February 2004 (in Japanese)

[5] K. Maekawa, A. Pimanmas and H. Okamura: Nonlinear Mechanics of Reinforced Concrete, SPON Press (Lonon), 2003

[6] J.M. Woods, P.D. Kiousis, M.R. Ehsani, H. Saadatmanesh and W. Fritz: Bending ductility of rectangular high strength concrete columns, Engineering Structures, Vol. 29, pp. 1783-1790, 2007

[7] S.-K. Hwang and H.-D. Yun: Effects of transverse reinforcement on flexural behavior of high strength concrete columns, Engineering Structures, Vol. 26, pp. 1-12, 2004